Available online at www.sciencedirect.com
SCIENCE DIRECT
Polymer 47 (2006) 2830–2838
polymer
www.elsevier.com/locate/polymer

Rubber toughening of nylon 6 nanocomposites

Young-Cheol Ahn [a], D.R. Paul [b,*]

[a] Department of Chemical Engineering, Kyungnam University, Masan, Kyungnam 631-701, Korea
[b] Department of Chemical Engineering, University of Texas at Austin, Austin, TX 78712, USA

Received 20 December 2005; received in revised form 14 February 2006; accepted 15 February 2006
Available online 13 March 2006

Abstract

The rubber toughening of nylon 6 nanocomposites prepared from an organoclay was examined as a means of balancing stiffness/strength versus toughness/ductility. Nine different formulations varying in montmorillonite, or MMT, and maleated ethylene/propylene rubber or EPR-*g*-MA rubber content were made by mixing of nylon 6 and organoclay in a twin screw extruder and then blending the nanocomposites with the rubber in a single screw extruder. In this sequence, the MMT platelets were efficiently dispersed in the nylon 6 matrix. The MMT platelets did not penetrate into the rubber phase. The addition of clay affected the dispersion of the rubber phase resulting in larger and more elongated rubber particles. The tensile properties and impact strength of these toughened nanocomposites are discussed in terms of the MMT and rubber contents and morphology. There is a clear trade-off between stiffness/strength versus toughness/ductility.

Keywords: Polyamide; Nanocomposite; Toughening

1. Introduction

Toughening of polyamides typically involves melt blending with a maleated elastomer wherein the grafted maleic anhydride readily reacts with the amine end groups of the polyamide to form a graft copolymer that strengthens the interface between the two phases and controls the morphology [1–7]. The size of the rubber particles in the blend is reduced because of the reduction in the particle–particle coalescence rate during melt mixing [8,9]. Rubber particle size is a key issue in achieving super-toughness of polyamides; generally, there are both lower and upper limits on particle size for optimum toughening depending on the polyamide type and molecular weight in addition to the rubber type [3,10–12]. It was shown that the rubber particle size should be generally controlled between 1 and 0.1 μm to give super-tough polyamide materials; these upper and lower critical particle sizes are known to depend on the molecular weight for nylon 6. The low temperature toughness of polyamide blends with styrene/hydrogenated butadiene triblock copolymers, SEBS, and ethylene/propylene random copolymers, EPR type elastomers depends on the molecular weight of nylon 6 and the type of elastomer [13]. The ductile to brittle transition temperature of such blends decreases as the molecular weight of the nylon 6 matrix increases and it can reach values as low as −50 °C for blends with maleated EPR elastomers or a block copolymer of low styrene content. Details of the fracture toughness of nylon 6 blends with maleated EPR rubber can be found in the literature [14].

Engineering polymers are often reinforced with glass fibers to obtain increased mechanical stiffness and strength; however, reinforcement with glass fibers, leads to reduced ductility and impact resistance. In some cases, it is useful to combine reinforcement with rubber toughening to balance end use performance. For glass–fiber reinforced, rubber-toughened nylon 6, the effects of glass fiber surface chemistry, glass fiber and rubber content, rubber particle size and rubber type on the impact and mechanical properties have been studied in detail [15–18]. Recently, there has been considerable interest in reinforcing polymeric materials using nanometer-sized particles with a high aspect ratio, i.e. nanocomposites. Fujiwara and Sakamoto [19] of the Unitika Co. described the first organoclay hybrid polyamide nanocomposite in 1976. One decade later, a research team from Toyota disclosed improved methods for producing nylon 6–organoclay nanocomposites using in situ polymerization similar to the Unitika process [20–23]. Vaia et al. proposed producing polymer nanocomposites by melt blending [24–27] which has great appeal since a conventional melt compounding process for forming nanocomposites would greatly expand the commercial

* Corresponding author. Tel.: +1 512 471 5392; fax: +1 512 471 0542.
E-mail address: drp@che.utexas.edu (D.R. Paul).

0032-3861/$ - see front matter © 2006 Elsevier Ltd. All rights reserved.
doi:10.1016/j.polymer.2006.02.074

opportunities for nanocomposites. Recently, there have been many studies reported on formation of nanocomposites by melt compounding [28–37]. The degree of exfoliation of the organoclay in a given polymer is strongly affected by the conditions of mixing, i.e. the viscosity of the matrix fluid, shear rate, residence time [32–34], and the structure of the organoclay [35].

The modulus of nanocomposites can be significantly increased compared to the neat nylon 6 [32,35] at low filler loadings, but the Izod impact strength is decreased and the ductile–brittle transition temperature is sharply increased as the content of nanosized particles is increased [32]. The use of nanocomposites can be limited by these losses in toughness; therefore, rubber toughening of nanocomposites becomes an interesting avenue to consider. The rubber toughening process used for neat nylon 6 and glass fiber/nylon 6 composites can also be applied for nanocomposites and is beginning to attract some interest [38–43]. This paper reports on a preliminary exploration of the rubber toughening of nylon 6 nanocomposites to better understand the balance of stiffness and toughness that can be achieved especially at low temperatures which is best expressed in terms of a ductile-to-brittle transition temperature.

2. Experimental

2.1. Materials

The nylon 6 used in this study was Capron B135WP from Honeywell (formerly AlliedSignal) with a number average molecular weight of 29,300 and a melt flow index of 1.2. The organoclay was Cloisite 30B supplied by Southern Clay Products. The montmorillonite (MMT) used to form this organoclay is refined from a Wyoming bentonite with a cation exchange capacity of 92 mequiv./100 g. Cloisite 30B is treated with 90 mequiv./100 g clay of Ethoquad T12, methyl bis-2-hydroxyethyl tallow quaternary ammonium chloride. The rubber used for toughening the nylon 6 nanocomposites was an ethylene–propylene random copolymer grafted with maleic anhydride (EPR-*g*-MA) obtained from ExxonMobil Chemical Company which contains 43 wt% ethylene, 57 wt% propylene, and 1.14 wt% grafted maleic anhydride.

2.2. Processing

The formation of the rubber toughened nylon 6 nanocomposites involved the following sequence of operations: first, melt compounding of the organoclay and nylon 6 to make a nanocomposite, and second, melt compounding of the nanocomposite with EPR-*g*-MA for toughening of the nanocomposite. The nanocomposites were prepared using a Haake co-rotating intermeshing twin screw extruder with 30 mm diameter screws having a centerline spacing of 26 mm and a screw length of 305 mm. The screw configuration contains two kneading disc blocks located at 37 and 127 mm, respectively, from the hopper. Both kneading disc blocks consist of one right-handed medium-pitched ($L/D=1$) and one left-handed medium-pitched ($L/D=1$) kneading disc elements and one mixing ring. The processing temperature was set at 240 °C and the screw revolution speed was fixed at 280 rpm. The organoclay powder and nylon 6 pellets were premixed in a tumbler and fed to the twin screw extruder using a microfeeder at the rate of 980 g/h. Prior to the melt processing, the pellets of neat nylon 6 were dried in a vacuum oven at 80 °C for a minimum of 16 h to satisfy the moisture content requirement of less than 0.2% for melt processing of nylon 6.

Blending of the nanocomposite with EPR-*g*-MA was carried out in a Killion single screw extruder having 25.4 mm diameter screw with an intensive mixing heads and a 762 mm screw length. The processing temperature was set at 240 °C and the screw speed was fixed at 40 rpm. Prior to the compounding, the pellets of nanocomposites were vacuum dried under the same condition as that for the neat nylon 6 and the EPR-*g*-MA pellets were dried in a hot air oven at 60 °C for several hours. Then, the two materials were mixed in a tumbler and supplied to the hopper of the extruder to obtain the rubber-toughened nanocomposites.

The extruded pellets of rubber-toughened nylon 6 nanocomposites were vacuum dried again in the similar manner before injection molding of the tensile and Izod impact specimens. The standard 0.318 cm (0.125 in.) thick tensile (ASTM D638 type I) and Izod (ASTM D256) bars were prepared using an Arburg Allrounder 305-210-700 injection molding machine. The barrel temperature was set to increase stepwise from 240 (hopper) to 270 °C (nozzle) with the mold temperature at 80 °C. An injection pressure of 70 bar and a holding pressure of 35 bar were used. A holding time of 9.0 s was needed to keep the materials in the cavity pressurized until cooling sealed the gate.

There are numerous other protocols that could be used to combine nylon 6, the organoclay and the maleated elastomer. The method used here was selected because it offers the best strategy for selectively placing the organoclay in the nylon 6 phase and not in the elastomer phase. Placement of the organoclay in the elastomer particles would not contribute as much to the overall modulus as having this reinforcement effect in the matrix phase and would diminish the toughening effect of the elastomer, particularly at low temperatures, by increasing its modulus. Thus, the best balance of stiffness and toughness dictates having the reinforcement in the matrix and not the dispersed phase. In commercial practice, one might use a twin screw extruder with multiple feed ports such that this same sequence of component addition could be achieved in a single step continuous process. In the absence of such an extruder, a two step process is the best route to the desired morphology.

2.3. Mechanical testing

Tensile tests were performed according to ASTM D638 using an Instron 1137, with an extensometer, upgraded with a computerized data acquisition system. Modulus and yield strength were measured at a crosshead speed of 0.51 cm/min. Elongation at break was measured at a crosshead speed of

5.1 cm/min using a value of 5.1 cm for the gauge length. Tensile data reported here are averages for seven specimens; standard deviations were less than 5% for modulus, 2% for yield strength and 20% for elongation at break.

Notched Izod impact strength was measured using a TMI pendulum type impact tester equipped with an insulated chamber for heating and cooling of the specimens. Eight specimens were tested for each composition and averages of the data are reported; standard deviations were less than 10% outside of the ductile to brittle transition region. All specimens were kept in a sealed desiccator under vacuum for 24 h before mechanical property measurements were performed.

2.4. Transmission electron microscopy (TEM)

Samples for TEM analysis were taken from the center region of a 13 cm Izod bar in three planes that are normal to (1) the flow direction, (2) the surface direction, and (3) transverse direction. Ultra thin sections of 45 nm thickness were cryogenically cut with a diamond knife at a temperature of −40 °C using a Reichert–Jung Ultracut E microtome. Mesa-cut sections were collected on a 300 mesh copper TEM grid and examined using a JEOL 2010 TEM with a LaB_6 filament at an accelerating voltage of 120 V. Specimens for observing rubber particle size were stained with 2% aqueous solution of phosphotungstic acid for 30 min.

2.5. Particle size analysis

Rubber particle size analysis was performed using the image measuring and processing software TDI Scope Eye®. The TEM photomicrographs were taken from the direction transverse to the flow and the negative films were scanned to get a digital image. The rubber particles were sometimes slightly extended in the flow direction relative to the transverse direction. The longitudinal dimension and the dimension perpendicular to the major direction were measured and their averages were calculated. Typically over 200 particles and several fields of view were analyzed. Because of non-spherical nature of the particles, no corrections were attempted to convert the apparent dimensions to the true dimensions [44–46].

3. Morphology

As mentioned earlier, the rubber toughened nylon 6 nanocomposites were prepared by compounding nylon 6 with organoclay to make a nanocomposite and the blending with maleated EPR rubber. Materials containing two levels of montmorillonite and two levels of rubber were selected for this study to give a total of nine materials including the unmodified nylon 6. For convenience, the amount of rubber and MMT (not organoclay) are expressed in terms of one hundred parts of nylon 6, or pph, rather than the total mass of the toughened nanocomposites; the compositions are expressed as a ratio of nylon 6/MMT/EPR-*g*-MA, that is, 100/*x*/*y*. The compositions of the nine materials prepared for this study are summarized in Table 1. The montmorillonite content was measured after incineration of the nanocomposite. The content of nylon 6 was obtained by subtracting the calculated content of organoclay in the nanocomposite. The organoclay consists of 27% by weight of the quaternary ammonium surfactant and 73% of montmorillonite clay.

These nanocomposites were used to form each of the rubber toughened formulations by mixing with EPR-*g*-MA in the Killion single screw extruder at a fixed processing temperature of 240 °C and screw rpm. The flow rate and residence time of the rubber-toughened nanocomposites were measured and are shown as functions of *x* and *y* in the composition 100/*x*/*y* of nylon 6/MMT/EPR-*g*-MA in Table 2. There are some slight variations with *x* and *y* in the average flow rate of ∼35.0 g/min and the average residence time of ∼1.7 min with standard deviations of 2.3 g/min and 0.1 min, respectively. These small variations in flow rate and residence time should not significantly affect the organoclay exfoliation or the rubber particle size.

Fig. 1 shows the clay platelets are generally well dispersed in the nylon 6 nanocomposites prepared in this study, see Fig. 1(a); however, there are some particles that consist of several platelets. The nanoparticles are generally oriented in the flow direction as shown in Fig. 1(b). It is interesting to imagine that the clay platelets may penetrate or intrude into the EPR rubber particles. However, this was never observed as shown in Fig. 1(c) where it is seen that the clay remains in the nylon 6 matrix. This may be due to the two-step process used. On the other hand, the rubber particles seem to affect the alignment of clay platelets in the immediate vicinity.

Table 1
Composition of rubber-toughened nylon 6 nanocomposites expressed in terms of the mass ratio of the components nylon 6/MMT/EPR-*g*-MA on the basis of one hundred parts of nylon 6, i.e. 100/*x*/*y*

		MMT content in nanocomposite[a]		
		0 wt%	3.2 wt%	6.5 wt%
Rubber content based on blend with nylon 6	0 wt%	$x=0$, $y=0$	$x=3.3$, $y=0$	$x=7.1$, $y=0$
	10 wt%	$x=0$, $y=11.1$	$x=3.3$, $y=11.1$	$x=7.1$, $y=11.1$
	20 wt%	$x=0$, $y=25$	$x=3.3$, $y=25$	x=7.1, y=25

[a] This MMT content was measured after incineration. MMT is added as organoclay, 27% of which is quaternary ammonium. Therefore, the content of organoclay must be subtracted from nanocomposite to obtain the content of nylon 6.

Table 2
Flow rate and residence time of rubber-toughened nylon 6 nanocomposites in the single screw extruder expressed as a function of x and y in the composition 100/x/y of nylon 6/MMT/EPR-g-MA

		$x=0$	$x=3.3$	$x=7.1$	Average	σ_n
Flow rate (g/min)	$y=0$	33.7	33.0	30.0	32.2	1.6
	$y=11.1$	37.7	37.0	36.3	37.0	0.6
	$y=25$	34.9	35.9	36.6	35.8	0.7
Residence time (min)	$y=0$	1.71	1.75	1.92	1.79	0.09
	$y=11.1$	1.53	1.56	1.59	1.56	0.02
	$y=25$	1.65	1.60	1.57	1.61	0.03

Other TEM photomicrographs of rubber toughened nylon 6 nanocomposites are shown in Figs. 2 and 3. In the case of rubber blends with neat nylon 6 most of the rubber particles are relatively small and of ellipsoidal shape. But the rubber particles in the nylon 6 nanocomposites seem somewhat larger and have a more extended ellipsoidal shape. These are interesting observations since increasing the matrix melt viscosity by increasing its molecular weight leads to smaller rubber particle sizes [11]. Nylon 6 nanocomposites have higher melt viscosity than neat nylon 6 because of the reinforcing effects by the silicate nanoparticles. Thus, one might expect that the rubber particles in the nylon 6 nanocomposites would be smaller in size when compared to the neat nylon 6, particularly since it has recently been proposed that the presence of clay particles retard the rate of coalescence of a dispersed polymer phase [42,43,47]. However, rubber particles in the nylon 6 nanocomposites appear to be larger and more extended in shape than those in rubber blends with neat nylon 6. The reason for this phenomenon is not understood at present but clearly deserves a deeper investigation, but this is beyond the scope of the current effort. We have observed in other systems more elongated rubber particles in the presence of clay particles; however, the rubber particles were generally smaller when clay was present [42]. In that case, the rubber particles were not grafted to the matrix as is the case here. Clearly, a first step in understanding this behavior would be to explore the effect of the processing sequence.

The distribution of longitudinal and transverse dimensions of the rubber particles were quantified by image analysis, and the weight-average particle dimensions were calculated from the size distribution as follows [11,45]

$$\bar{d}_w = \frac{\sum n_i d_i^2}{\sum n_i d_i} \quad (1)$$

where n_i is the number of rubber particles within the length range i. The results are summarized in Table 3. The weight average particle size is frequently used for correlating the toughness of polymer blends and allows comparisons with values reported in the literature [11]. For nylon 6 blends with no clay, the weight-average dimensions of the rubber particles were 0.24 μm in the longitudinal direction and 0.13–0.16 μm in the transverse direction. These dimensions fall within the particle size range of 0.1–1 μm where toughening is effective; however, there is relatively little information on how rubber particle shape affects toughening. On the other hand, in the

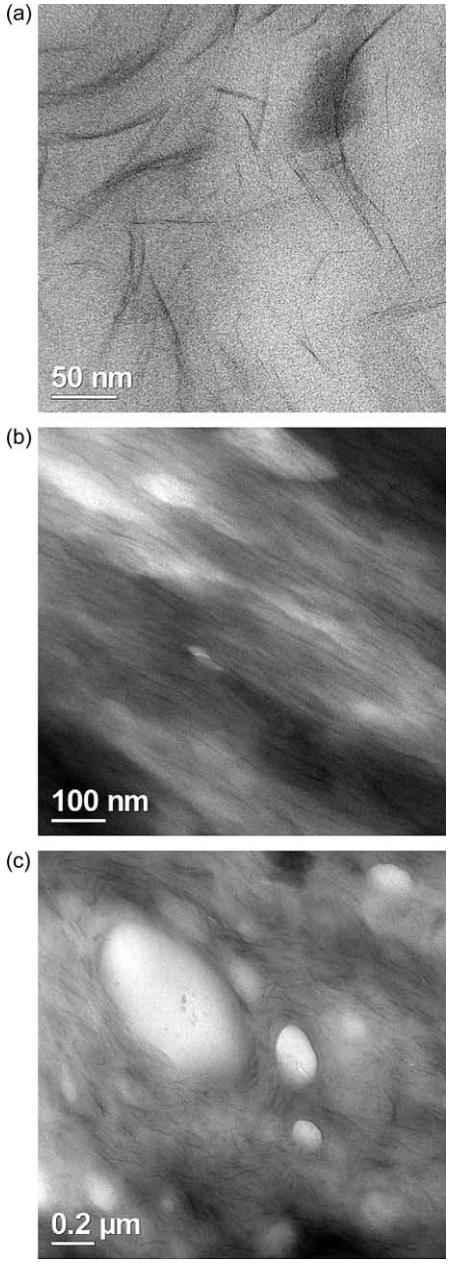

Fig. 1. Transmission electron micrographs of nanocomposites with the compositions nylon 6/MMT/EPR-g-MA of (a) 100/3.3/0 as seen prior to injection molding so platelets are not aligned, (b) 100/7.1/0 viewed in the transverse direction of an injection molded sample to reveal platelet orientation, and (c) 100/3.3/11.1 viewed in the flow direction of an injection molded specimen.

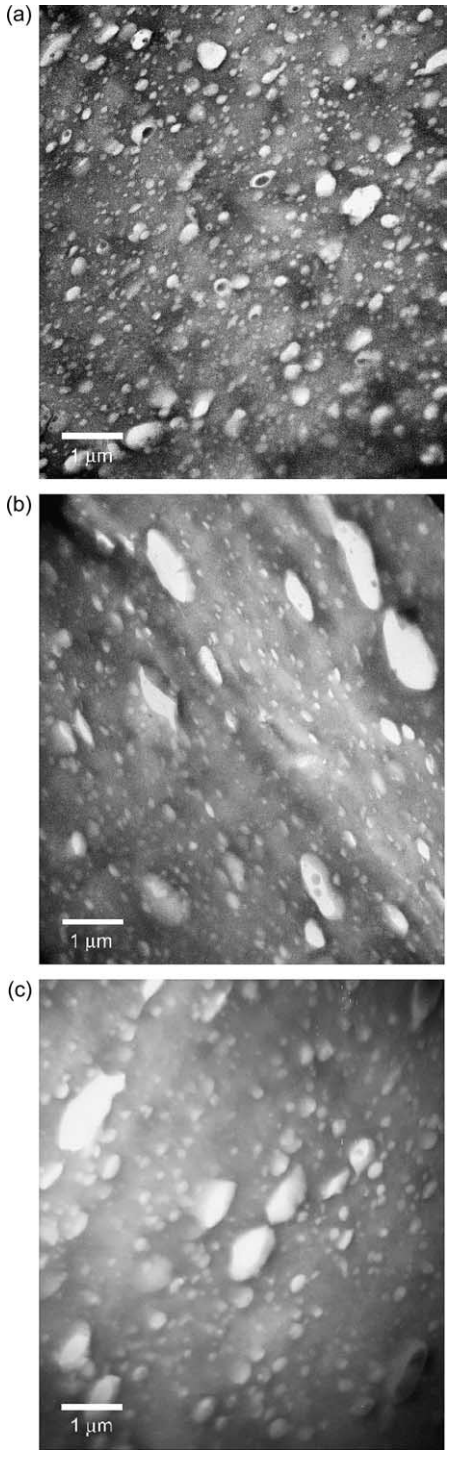

Fig. 2. Transmission electron micrographs of rubber toughened nylon 6 nanocomposites with the compositions nylon 6/MMT/EPR-*g*-MA of (a) 100/0/11.1, (b) 100/3.3/11.1, and (c) 100/7.1/11.1.

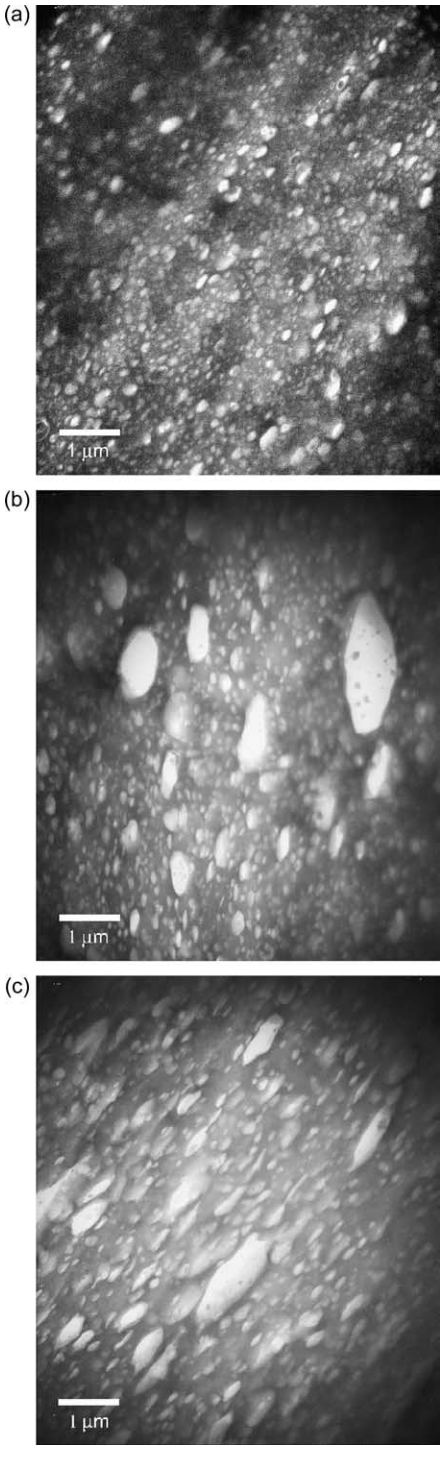

Fig. 3. Transmission electron micrographs of rubber toughened nylon 6 nanocomposites with the compositions nylon 6/MMT/EPR-*g*-MA of (a) 100/0/25, (b) 100/3.3/25, and (c) 100/7.1/25.

nylon 6 nanocomposites the weight-average dimensions of rubber particles were 0.41–0.52 μm in the longitudinal direction and 0.19–0.23 μm in the transverse direction, respectively. These dimensions again fall within the rubber-toughening particle size range even though they are larger than the former case and the shape is more extended. To understand the consequences of these rubber particle size and shape changes on the toughness observed would require a much more detailed investigation than was possible in this preliminary study.

4. Tensile properties

The tensile properties of the rubber toughened nylon 6 nanocomposites including modulus, yield stress, and elongation

Table 3
Dimensions of rubber particles in the rubber-toughened nylon 6 nanocomposites expressed as a function of x and y in the composition 100/x/y of nylon 6/MMT/EPR-g-MA

		$x=0$	$x=3.3$	$x=7.1$
$d_{w,L}$ (μm)	$y=11.1$	0.24	0.48	0.41
	$y=25$	0.24	0.47	0.52
$d_{w,T}$ (μm)	$y=11.1$	0.16	0.23	0.23
	$y=25$	0.13	0.22	0.19

$d_{w,L}$, weight-average longitudinal dimension of rubber particles; $d_{w,T}$, weight-average transversal dimension of rubber particles.

Table 4
Tensile properties of rubber-toughened nylon 6 nanocomposites expressed as a function of x and y in the composition 100/x/y of nylon 6/MMT/EPR-g-MA

		$x=0$	$x=3.3$	$x=7.1$
E (GPa)	$y=0$	2.92±0.08	4.44±0.12	5.53±0.07
	$y=11.1$	2.44±0.02	3.33±0.05	4.50±0.15
	$y=25$	2.08±0.09	2.59±0.08	3.49±0.10
σ_{yield} (MPa)	$y=0$	73.9±1.1	91.7±1.2	100.1±0.7
	$y=11.1$	60.3±0.6	67.8±0.6	76.0±0.7
	$y=25$	50.5±0.3	53.2±0.3	60.6±0.3
ε_b (%)	$y=0$	108±47	35±10	10±2
	$y=11.1$	108±55	38±14	25±3
	$y=25$	114±57	45±6	28±2

E, elastic modulus; σ_{yield}, yield strength; ε_b, percent elongation at break.

at break are summarized in Table 4. The tensile modulus of nylon 6 nanocomposites without rubber increased almost linearly from 2.92 to 4.44 to 5.53 GPa as the composition of montmorillonite (MMT) was increased from 0 to 3.3 to 7.1 pph of nylon 6; these compositions correspond to 0, 3.2 and 6.5 wt% of MMT, respectively, based on total mass. The current trends correspond well with the results of Fornes et al. [35]; however, the magnitudes of the moduli in this work are a little larger than those in the prior study. The differences are believed to be due to differences in injection molding conditions used in the two studies. The modulus of blends without clay linearly decreased from that of neat nylon 6, 2.92 to 2.08 GPa as the rubber content was increased to 25 pph parts nylon 6 or 20 wt% rubber based on total mass. The addition of both rubber and organoclay has compensating effects on the tensile modulus that more or less parallel the trends of adding just clay or rubber as seen in Table 4.

The yield stress values for each material are listed in Table 4. As expected the yield strength decreases on addition of rubber but increases on addition of clay.

The elongation at break decreases significantly with addition of clay as reported previously. Adding rubber increases the elongation at break but only modestly. All formulations containing clay have lower values of elongation at break than nylon 6 as may be seen in Table 4.

5. Impact behavior

The rubber particle size or inter-particle distance plays a key role in toughening of plastic materials as suggested by Wu [1]. The lower and upper limits of the weight-average diameter of rubber particles were shown to be 0.1 and 1 μm for nylon 6 by Oshinski et al. [12]. In this study, the weight-average dimensions of rubber particles in the longitudinal and transverse directions were well managed to be within this range as shown in Table 3. Therefore, the current blends of nylon 6 with EPR-g-MA show good toughening. If we regard the matrix as the nanocomposite, these limits may be different; however, to establish this would require a more extensive study than is currently possible. Izod impact strength values for rubber-toughened nylon 6 nanocomposites are summarized in Table 5 as functions of x and y in the composition 100/x/y of Nylon 6/MMT/EPR-g-MA. For the case of neat nylon 6 ($x=y=0$), the impact strength is 63 J/m which decreases slightly to 45 J/m as MMT was added to the level of 7.1 pph. Addition of rubber in the absence of clay causes a large increase in the Izod value as expected [1–4]. When the rubber content is 11.1 pph, the addition of clay causes a much stronger reduction of the Izod values. However, when the rubber content is 25 pph, addition of clay actually causes the room temperature Izod to increase to a very large value and then to decline some as more clay is added. To understand the effects shown here, it is important to remember that the Izod value is the area under a force–displacement curve. While addition of clay reduces the extent of plastic deformation, at least in tensile tests as shown in Table 4, it also increases the stiffness and yield strength or the force levels. In addition, one needs to understand where the ductile-to-brittle transition temperature for each material lies with respect to room temperature as discussed next in terms of plots of Izod versus temperature, see Figs. 4–9.

In the absence of rubber, nylon 6 shows a ductile region at temperatures above 50 °C and a brittle region at temperatures below 50 °C as seen in Fig. 4. This ductile-to-brittle transition corresponds to the glass transition of the dry-as molded nylon 6. Addition of clay particles increases the ductile–brittle transition temperature and makes the nylon 6 slightly more brittle below this transition. The addition of rubber in the absence of clay greatly lowers the ductile–brittle transition temperature and has the effect of increasing toughness for a given temperature like 25 °C. At the rubber content of 11.1 pph, the Izod shows a plateau at around room temperature with a value of about 600 J/m. The ductile–brittle transition temperature for this composition is 5 °C. In the brittle region at temperatures below −5 °C, however, the impact strength has a value more than 200 J/m which is three times that of neat nylon 6 and might be considered tough enough for some applications. There is another plateau above 40 °C that results from the glass transition of nylon 6. When the rubber content is 25 pph, the

Table 5
Izod impact strengths of rubber-toughened nylon 6 nanocomposites expressed as a function of x and y in the composition 100/x/y of nylon 6/MMT/EPR-g-MA in units of J/m.

	$x=0$	$x=3.3$	$x=7.1$
$y=0$	63±13	49±5	45±7
$y=11.1$	603±15	151±10	106±10
$y=25$	565±24	951±23	620±116

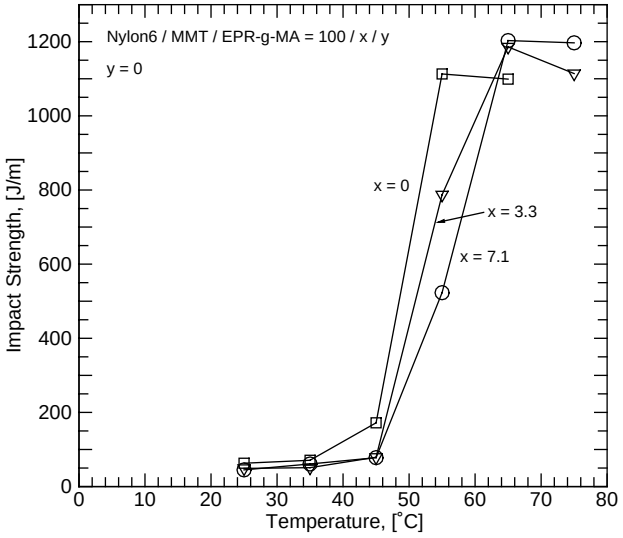

Fig. 4. Effects of MMT content on the impact strength of nylon 6 nanocomposites versus temperature when the rubber content is zero.

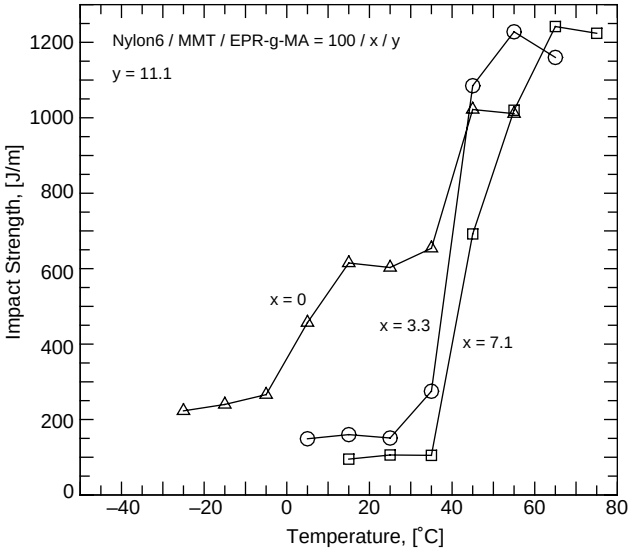

Fig. 6. Effect of MMT content on the impact strength of rubber toughened nylon 6 nanocomposites versus temperature when the rubber content is 11.1 pph.

ductile–brittle transition temperature is decreased to −25 °C. In the ductile region, the impact strength reaches values of about 800 J/m at 0 °C and then decreases to about 500 J/m as the temperature is increased to 35 °C. These complex trends reflect multiple issues. One might think of two ductile-to-brittle transitions. The lower one is the result of the rubber toughening of the nylon 6 below its glass transition temperature; this depends on rubber content and morphology. The other transition is where the nylon 6 goes from being glassy to rubbery in the amorphous phase and leads to a strong ductile-to-brittle transition even in the absence of rubber. The fact that the Izod values may show a plateau or even decrease as temperature is increased between these two limits most likely reflects a reduction in yield strength with temperature. Recall that the Izod value reflects the area under a force–displacement, and if the force is reduced because of a lower yield stress, then the area will be reduced.

Fig. 6 shows the effect of MMT content on impact strength as a function of temperature when the rubber content is 11.1 pph. Addition of clay suppresses the plateau seen for the case of no clay that lies in between the transitions caused by rubber toughening and by the matrix T_g; thus, the composites are brittle at temperatures below 35 °C. Similar effects are seen in Fig. 7, where the rubber content is 25 pph. In this case, however, the suppression effect is not as great as in the case of $y = 11.1$ pph; the higher rubber content significantly lowers the ductile–brittle transition temperature due to rubber toughening.

The effects of rubber content on the impact strength versus temperature relationship for nylon 6 nanocomposites are

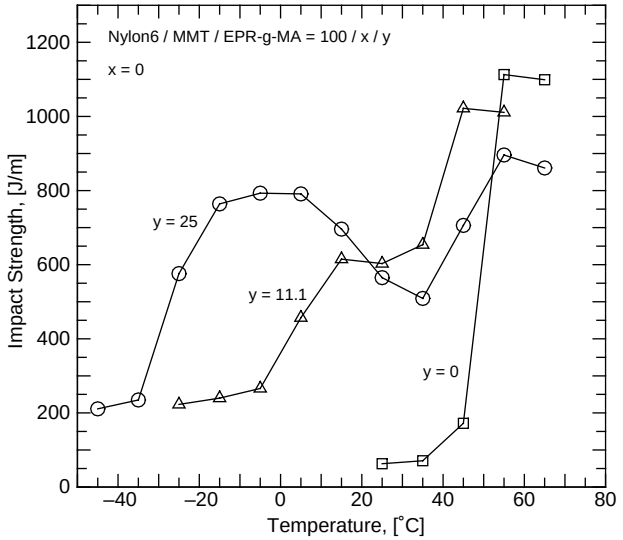

Fig. 5. Effect of rubber composition on the impact strength of rubber blends of nylon 6 versus temperature when the MMT content is zero.

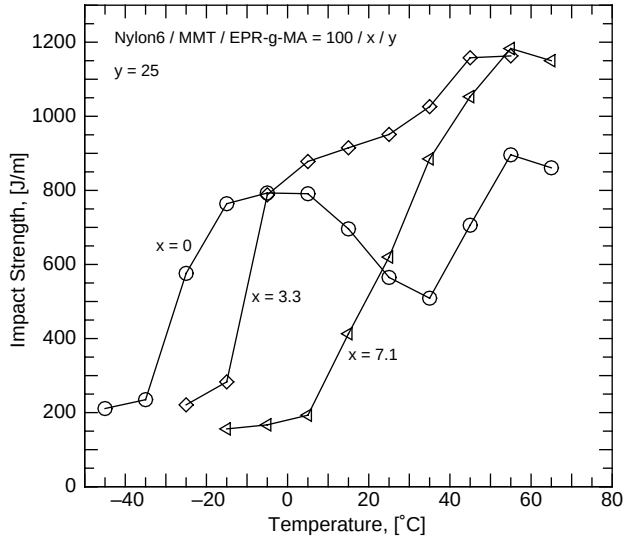

Fig. 7. Effect of MMT content on the impact strength of rubber toughened nylon 6 nanocomposites versus temperature when the rubber content is 25 pph.

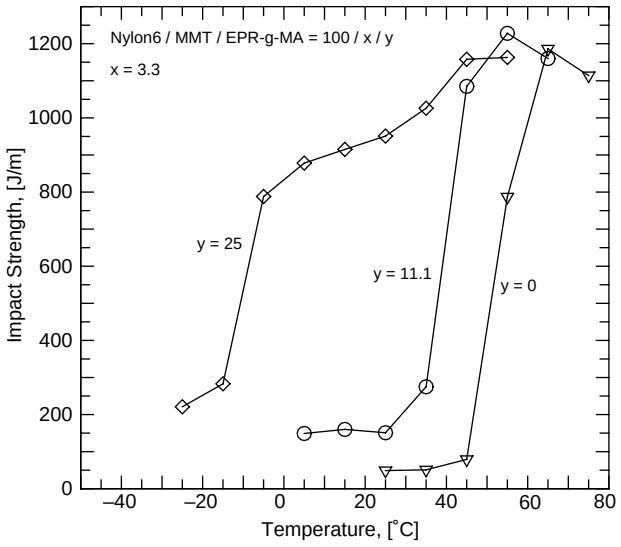

Fig. 8. Effect of rubber content on the impact strength of rubber toughened nylon 6 nanocomposites versus temperature when the MMT content is 3.3 pph.

shown more clearly in Figs. 5, 8 and 9. When the MMT is 3.3 pph, a rubber content of 25 pph is needed to obtain a plateau of the impact strength over some range of temperature as shown in Fig. 8. On the other hand, no plateau is seen for the case of $x=7.1$ pph even for a rubber content of 25 pph as may be seen in Fig. 9. In the discussion of Fig. 5, it was noted that a rubber content of 11.1 pph was needed to see a plateau in the absence of MMT. As clay is added, even higher levels of rubber are needed to have a plateau in the impact strength versus temperature relationship. Table 6 summarizes the ductile–brittle transition temperature as a function of clay and rubber contents.

The impact and tensile results presented here allows one to assess what would be a good combination of MMT and rubber

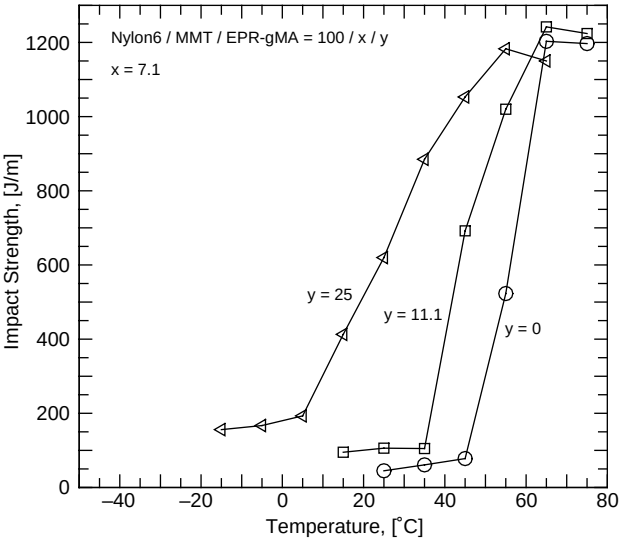

Fig. 9. Effects of rubber content on the impact strength of rubber toughened nylon 6 nanocomposites versus temperature when the MMT content is 7.1 pph.

Table 6
Ductile–brittle transition temperatures (°C) of rubber-toughened nylon 6 nanocomposites expressed as a function of x and y in the composition 100/x/y of nylon 6/MMT/EPR-g-MA

	$x=0$	$x=3.3$	$x=7.1$
$y=0$	50	55	55
$y=11.1$	5	40	40
$y=25$	−25	−10	20

contents to best meet the needs of a given material application. As expected, there are clearly tradeoffs to be made between stiffness and strength versus toughness.

6. Conclusions

In this study, rubber toughening of nylon 6 nanocomposites was examined in terms of impact strength, ductile–brittle transition temperature, and tensile properties. Nine different compositions varying in the content of MMT and EPR-g-MA rubber, i.e. x and y in the composition 100/x/y of nylon 6/MMT/EPR-g-MA, were prepared by mixing nylon 6 with MMT in a twin screw extruder and then blending the nanocomposites with the rubber in a single screw extruder. In this sequence, the MMT platelets were efficiently dispersed in the nylon 6 matrix. It was shown that the MMT platelets did not penetrate into the rubber phase. This is the morphology desired for an optimal balance of stiffness and toughness. The presence of the clay platelets appears to affect the dispersion of the rubber phase resulting in larger and elongated rubber particles. The tensile properties of the rubber toughened nylon 6 nanocomposites were shown as a function of the values of x and y of the formulation. The impact strength versus temperature relationships were examined to determine the ductile–brittle transition temperatures as a function of MMT and rubber contents. There is clearly a trade-off between properties like stiffness and strength versus ductility and toughness as might be expected.

Rubber particles appropriately dispersed within a neat nylon 6 matrix increase toughness via cavitation which relieves the triaxial stress state ahead of the advancing crack tip and allows the nylon 6 matrix to shear yield and thereby dissipate more energy. The presence of clay platelets probably does not alter the qualitative features of this mechanism; however, quantitative details may well be changed. One could imagine that the reinforcing effect of the clay platelets mechanically constrains the matrix and limits the shear yielding process. Future studies should seek to better understand how the presence of the clay platelets affects the morphology of the rubber phase and the optimum range of rubber particle sizes for toughening. In addition, it would be useful to better understand the extent to which the presence of the rubber particles affect the morphology of the nanocomposite matrix phase particularly the orientation of the clay platelets as this is an important factor affecting modulus.

Acknowledgements

This study was supported by the 2003 Kyungnam University Research Grants for Sabbatical Leave.

References

[1] Wu S. Polymer 1985;26:1855.
[2] Wu S. Polymer Eng Sci 1987;27:335.
[3] Oshinski AJ, Keskkula H, Paul DR. Polymer 1992;33:268.
[4] Oshinski AJ, Keskkula H, Paul DR. Polymer 1992;33:284.
[5] Fayt R, Jerome R, Teyssie R. ACS Symp Ser 1989;395:38.
[6] Lambla M, Yu RX, Lorek S. ACS Symp Ser 1989;385:67.
[7] Cimmino S, Copolla F, D'Orazio L, Greco R, Maglio G, Malinconinco M, et al. Polymer 1986;27:1874.
[8] Majumdar B, Keskkula H, Paul DR. Polymer 1994;35:1386.
[9] Sundararaj U, Macosko CW. Macromolecules 1995;28:2647.
[10] Oostenbrink AJ, Molenaar LJ, Gaymans RJ. Polyamide–rubber blends: influences of very small particle sizes on impact strength; 1990. Poster given at sixth annual meeting of polymer processing society, Nice, France, 18–20 April.
[11] Oshinski AJ, Keskkula H, Paul DR. Polymer 1996;37:4891.
[12] Oshinski AJ, Keskkula H, Paul DR. Polymer 1996;37:4909.
[13] Oshinski AJ, Keskkula H, Paul DR. Polymer 1996;37:4919.
[14] Okada O, Keskkula H, Paul DR. Polymer 2000;41:8061.
[15] Laura DM, Keskkula H, Barlow JW, Paul DR. Polymer 2000;41:7165.
[16] Laura DM, Keskkula H, Barlow JW, Paul DR. Polymer 2001;42:6161.
[17] Laura DM, Keskkula H, Barlow JW, Paul DR. Polymer 2002;43:4673.
[18] Laura DM, Keskkula H, Barlow JW, Paul DR. Polymer 2003;44:3347.
[19] Fujiwara S, Sakamoto T. Japanese Kokai Patent Application No. 109998; 1976. Assigned to Unitika KK, Japan.
[20] Fukushima Y, Inagaki S. J Inclusion Phenom 1987;5:473.
[21] Okada A, Fukushima Y, Kawasumi M, Inagaki S, Usuki A, Sugiyama S, et al. United States Patent No. 4739007; 1988. Assigned to Toyota Motor Co., Japan.
[22] Kawasumi M, Kohzaki M, Kojima Y, Okada A, Kamigaito O. United States Patent No. 4810734; 1989. Assigned to Toyota Motor Co., Japan.
[23] Usuki A, Kojima Y, Kawasumi M, Okada A, Fukushima Y, Kurauch T, et al. J Mater Res 1993;8:1179.
[24] Vaia RA, Ishii H, Giannelis EP. Chem Mater 1993;5:1694.
[25] Vaia RA, Jandt KD, Kramer EJ, Giannelis EP. Macromolecules 1995;28: 8080.
[26] Vaia RA, Giannelis EP. Macromolecules 1997;30:7990.
[27] Vaia RA, Giannelis EP. Macromolecules 1997;30:8000.
[28] Maxfield M, Christiani BR, Murthy SN, Tuller H. United States Patent No. 5385776; 1995. Assigned to AlliedSignal Inc.
[29] Christiani BR, Maxfield M. United States Patent No. 5747560; 1998. Assigned to AlliedSignal Inc.
[30] Kawasumi M, Hasegawa N, Kato M, Usuki A, Okada A. Macromolecules 1997;30:6333.
[31] Liu L, Qi Z, Zhu X. J Appl Polym Sci 1999;71:1133.
[32] Cho JW, Paul DR. Polymer 2001;42:1083.
[33] Dennis HR, Hunter DL, Chang D, Kim S, White JL, Cho JW, et al. Polymer 2001;42:9513.
[34] Fornes TD, Yoon PJ, Keskkula H, Paul DR. Polymer 2001;42:9929.
[35] Fornes TD, Yoon PJ, Hunter DL, Keskkula H, Paul DR. Polymer 2002;43: 5915.
[36] Yoon PJ, Hunter DL, Paul DR. Polymer 2003;44:5323.
[37] Yoon PJ, Hunter DL, Paul DR. Polymer 2003;44:5341.
[38] Kelner I, Kotek J, Kapralkova L, Munteanu BS. J Appl Polym Sci 2005; 96:288.
[39] Tjong SC, Bao SP. J Polym Sci, Part B: Polym Phys 2005;43:585.
[40] Tjong SC, Bao SP, Liang GO. J Polym Sci, Part B: Polym Phys 2005;43: 3112.
[41] Dasari A, Yu A-A, Mai Y-W. Polymer 2005;46:5986.
[42] Lee H-S, Fasulo PD, Rodgers WR, Paul DR. Polymer 2005;46:11673.
[43] Mehta S, Mirabella FM, Rufener K, Bafna A. J Appl Polym Sci 2004;92: 928.
[44] Bach G. Qualitative methods in morphology. Berlin: Springer; 1967.
[45] Irani RR, Callis CF. Particles size: measurement, interpretation and application. New York: Wiley; 1963.
[46] Chamot EM, Mason CW. Handbook of chemical microscopy. London: Wiley; 1983.
[47] Khatua BB, Lee DJ, Kim HY, Kim JK. Macromolecules 2004;37:2454.